XLIII CILAMCE
21–25, November, 2022
FOZ DO IGUAÇU – PR – BRAZIL

Time domain aeroelastic analysis of clamped wings and determination of V-g-f plots using modal parameter identification

João Pedro Tavares Pereira dos Santos[1], Guilherme Ribeiro Begnini[2], Flávio Donizeti Marques[1]

[1]*Mechanical Engineering Department, São Carlos Engineering School of University of São Paulo*
Avenida Trabalhador são-carlense, 400 - Parque Arnold Schimidt, 13566-590, São Carlos/SP, Brazil
jptpsantos@usp.br, fmarques@sc.usp.br
[2]*Mechanical Engineering Department, Polytechnic School of Federal University of Bahia*
R. Prof. Aristídes Novis, 2 - Federação, 40210-630, Salvador/BA, Brazil
guilherme.begnini@ufba.br

Abstract. Aeroelastic analyses are performed either in time or frequency domains. Frequency domain analyses have the advantage of providing a fast computation of the flutter speed and are more widespread. Their results are presented in the so-called velocity-damping-frequency (V-g-f) plots, which shows the evolution of the natural frequency and damping ratio of each vibration mode as a function of airspeed. This way, the flutter speed (where zero damping occurs) can be determined with precision. On the other hand, time domain analyses allow the inclusion of different types of nonlinearities in the simulations, with the price of being more time consuming. Their results consist of time histories whose vibration amplitudes should be visually inspected to find a constant amplitude situation (zero damping condition). This paper presents time domain aeroelastic analysis of a set of rectangular cantilever plates with different aspect ratios that represent aircraft wings in a simplified way. Time domain results are then used to generate V-g-f plots through modal parameter identification. For the structural dynamics modeling, both the classical beam theory (Euler-Bernoulli) and the classical plate theory have been applied, and the natural frequencies and mode shapes were obtained via the Finite Element Method (FEM). For the aerodynamic modeling of the plates, the Unsteady Vortex Lattice Method (UVLM) was used, which is a three-dimensional aerodynamic model based on a potential flow formulation. The structural and aerodynamic models are coupled using a surface splines interpolation method, and the movement equation is solved iteratively on a time-domain basis, applying a predictor-corrector method. The frequency spectrum of each time response serves as input to the modal parameter identification method, which uses the Least Squares Complex Frequency estimator (LSCF). A stabilization chart is obtained based on the frequency and damping convergence criteria, thereby allowing the identification of the modal parameters. The structural and aeroelastic results of the plate, considering both beam theory and plate theory, are evaluated. It was possible to obtain very clear V-g-f plots, with a precise identification of flutter speeds, for all tested cases. The influence of the structural model on the flutter speed results was assessed.

Keywords: Aeroelasticity, Unsteady Vortex Lattice Method, Finite Element Method, System Identification, Flutter

1 Introduction

On the latest years, in searching for more efficiency and less fuel consuption, longer and more flexible wings have been developed, which reduces the induced drag. These characteristics increase the importance of aeroelastic analysis of these structures, which allows to determine how the oscillatory behavior will be in the presence of air flow.

For aeroelastic analysis, two distinct mathematical models must be coupled: one to represent the structural dynamics and other to represent the aerodynamics of the wing. The structural dynamics model aims to determine the natural frequencies and vibrational mode shapes, and the aerodynamic model aims to determine the loads acting on the structure. Coupling those two models, it's possible to solve the dynamic equations of motion and predict the oscillatatory behaviour of the wing.

The flutter analysis is a crucial step on the project and analysis of these high flexible aeronautic structures, and is the focus of this work. It consists in the prediction of the speed and frequency where is observed zero damping ratio, which are called the flutter frequency and speed. From that point, the system becomes unstable, and the structure is likely to fail. Thus, it is important to avoid this point.

The flutter analysis can be performed either in frequency or time domains. The advantage of the first one is that it provides faster computation of the flutter speed and is more widespread. The results are presented directly in the velocity-damping-frequency (V-g-f) plot, which allows the visualization of the evolution of the natural frequency and damping ratio of each vibration mode as function of the airspeed and, consequently, the precise prediction of the flutter speed. The time domain analysis is more time consuming, and it provides as results the time histories. The vibration amplitudes of the time responses have to be visually inspected to identify where a constant amplitude is observed (zero damping ratio). From the time domain results, it is possible to apply a modal parameter identification method to generate the V-g-f plots.

The interaction between a cantilevered flexible elastic plate and a uniform incompressible flow is an iconic subject in fluid–structure interaction. This configuration can, of course, be extended to more complex aerospace structures for predicting and avoiding aeroelastic instabilities in the real world. Simple systems, such as the rectangular plate, have received good attention in the literature. From that, this work proposes the aeroelastic analysis of a set of rectangular plates with different aspect ratios, which models, in a simplified way, a wing [1].

The aeroelastic model proposed here to analyze a set of rectangular cantilever plates is a time domain model, and the time histories are used to generate V-g-f plots through modal parameter identification. For the structural dynamics modelling, the Euler-Bernoulli beam model, and the classical plate theory, have been applied to determine the natural frequencies and mode shapes through the Finite Element Method (FEM). The Unsteady Vortex Lattice Method (UVLM) [2] was applied for the aerodynamic modelling, which is a three-dimensional aerodynamic model based on the potential flow theory. Both models are coupled together using a surface splines interpolation method, and the movement equation is solved iteratively on a time-domain basis, applying a predictor-corrector method. The frequency spectrum of each time response serves as input to the model parameter identification method, which uses the Least Squares Complex Frequency estimator (LSCF) [3]. The theory and the results obtained are presented on the next sections.

2 Structural Dynamics

For the structural part of the aeroelastic analysis, the Finite Element Method was applied, considering both Euler-Bernoulli beam elements and plate elements. The theory regarding the beam formulation is presented by Cook and Saunders [4], Craig and Kurdila [5], Reddy [6] and Katsikadelis [7]. The plate formulation is presented by Gruppioni [8], and the plate FEM code developed in his work was given to use.

The wing structural response is assumed to be linear and without internal damping. The equation of motion for the structure discretized in N degrees of freedom (DOF) is shown in eq. (1), where $\boldsymbol{M}$ and $\boldsymbol{K}$ are $N \times N$ matrices, representing the mass and stiffness properties, and $\boldsymbol{x}(t)$, $\ddot{\boldsymbol{x}}(t)$ and $\boldsymbol{L}(\boldsymbol{x}, \dot{\boldsymbol{x}}, \boldsymbol{t})$ are $N \times 1$ vectors, representing the displacements, accelerations and external (aerodynamic) forces. The beam element have 12 DOF, and the $\boldsymbol{M}$ and $\boldsymbol{K}$ matrices are presented by Katsikadelis [7].

$$\boldsymbol{M}\ddot{\boldsymbol{x}}(t) + \boldsymbol{K}\boldsymbol{x}(t) = \boldsymbol{L}(\boldsymbol{x}, \dot{\boldsymbol{x}}, \boldsymbol{t}) \tag{1}$$

The natural frequencies (ω) and mode shapes ($\boldsymbol{\phi}_r$) of the undamped multiple degree of freedom system are obtained by solving the following eigenvalue problem

$$\left(\boldsymbol{K} - \omega^2 \boldsymbol{M}\right) \boldsymbol{\phi}_r = \boldsymbol{0} \tag{2}$$

The mode shapes can be arranged in a matrix, as seen in eq. (3). This matrix is called modal matrix and is used as a coordinate transformation matrix, according to eq. (4), where $\boldsymbol{\eta}(t)$ represents the structural displacements in a modal domain and can be interpreted as a vector of coefficients which determines the influence of each mode shape in the physical structural response.

$$\boldsymbol{\Phi} = [\boldsymbol{\phi}_1 \; \boldsymbol{\phi}_2 \; \boldsymbol{\phi}_3 \; \cdots \; \boldsymbol{\phi}_N] \tag{3}$$

$$\boldsymbol{x}(t) = \boldsymbol{\Phi}\boldsymbol{\eta}(t) = \sum_{r=1}^{N} \boldsymbol{\phi}_r \boldsymbol{\eta}_r(t) \tag{4}$$

As $\boldsymbol{\Phi}$ is constant in time, it's possible to write

$$\ddot{\boldsymbol{x}}(t) = \boldsymbol{\Phi}\ddot{\boldsymbol{\eta}}(t) \tag{5}$$

Substituting eq. (4) and eq. (5) in eq. (1) and pre-multiplying both sides by $\boldsymbol{\Phi}^T$, yields eq. (6), where $\boldsymbol{M}_m = \boldsymbol{\Phi}^T\boldsymbol{M}\boldsymbol{\Phi}$ and $\boldsymbol{K}_m = \boldsymbol{\Phi}^T\boldsymbol{K}\boldsymbol{\Phi}$ are named modal mass and modal stiffness matrices, respectively.

$$\boldsymbol{M}_m\ddot{\boldsymbol{\eta}}(t) + \boldsymbol{K}_m\boldsymbol{\eta}(t) = \boldsymbol{\Phi}^T L(x, \dot{\boldsymbol{x}}, t) \tag{6}$$

Due to the orthogonality properties of the mode shapes, one can prove that the matrices $\boldsymbol{M}_m$ and $\boldsymbol{K}_m$ are diagonal matrices. In addition, it is possible to normalize the eingenvectors in a form that $\boldsymbol{M}_m = I$, and then the division of both sides of eq. (6) by the matrix $\boldsymbol{M}_m$ yields eq. (7), where ω^2 is a diagonal matrix containing the squared natural frequencies.

$$\ddot{\boldsymbol{\eta}}(t) + \boldsymbol{\omega}^2\boldsymbol{\eta}(t) = \boldsymbol{\Phi}^T\boldsymbol{L}(\boldsymbol{x}, \dot{\boldsymbol{x}}, t) \tag{7}$$

In order to simplify the solution of eq. (7), it is useful to consider only a few natural modes to describe the structural response. Another important step of the aeroelastic analysis is the determination of the aerodynamic loads ($\boldsymbol{L}(\boldsymbol{x},\dot{\boldsymbol{x}},t)$). The aerodynamic model used here is the Unsteady Vortex Lattice Method (UVLM), described by Katz and Plotkin [2], which will be discussed on the next topic. Once those loads are determined, the structural and aerodynamic models must be coupled togheter.

3 Unsteady Vortex Lattice Method

The UVLM is am aerodynamic method based on the potential theory and on the resolutions of Laplace's equations, applying the potential flow. This method is a extremely useful tool to solve three-dimensional potential flow problems and to represent lifting surfaces. This surfaces, combined with the wake, are modelled through vortex rings elements.

The lifting surface, here the wing, is discretized in rectangular panels along the curvature line of the airfoil. Each vortex ring is associated to one of those panels. The rings connected to the lifting surface are called bound vortices. With the movement of the wing, more vortices are formed and the wake arises. In this work, the wake is considered free. Besides that, a normal vector is defined in each collacation point. Figure Fig. 1 describes this.

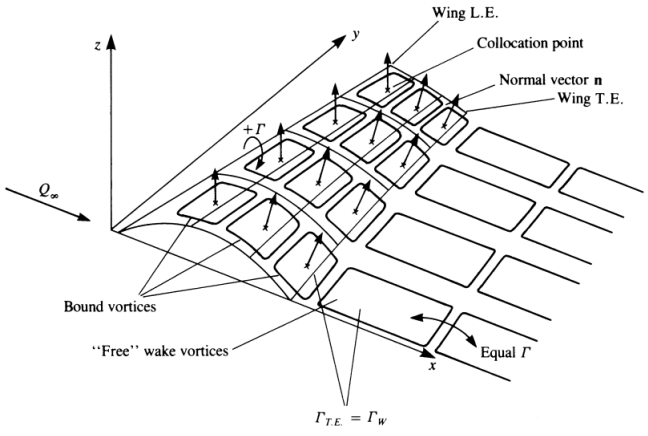

Figure 1. UVLM Wing and Wake Modelling

The UVLM is solved through an time iterative algorithm. In the beginning of the resolution of the aerodynamic problem, the vortex rings of the wake flow through the leading edge of the wing, and deforms according to the local flux. New rings are generated each time step, and the correspondent circulations

(Γ) are defined. It's important to emphasize that the circulation of the wake rings are equal to the ones of the trailing edge of the wing, which is described by

$$\Gamma_W = \Gamma_{T.E.} \tag{8}$$

To calculate the aerodynamic loads acting on the wing, It's necessary to solve the flow field, finding the circulation of the vortex rings linked to the wing panels. For this to be possible, the first step is to calculate the influence that each vortex ring exerts on the flow field, and, for this, the so-called Aerodynamic Influence Coefficients (AIC) are used. This coefficients are defined from the calculation of the induced velocity of each vortex segment of the ring on the collocation points.

The aerodynamic influence of each ring, here called a_{kl}, is defined by

$$a_{kl} = \mathbf{q}_{kl} \cdot \mathbf{n}_k \tag{9}$$

where a_{kl} is the influence of ring l on the collocation point k, $\mathbf{q}_{kl}$ is the induced velocity, found applying the Biot-Savart law, on the collocation point k by the vortex ring l and $\mathbf{n}_k$ is the normal vector of the ring l. Combining those aerodynamic influences on a matrix, the AIC is defined.

$$AIC = \begin{bmatrix} a_{11} & a_{12} & \cdots & a_{1m} \\ a_{21} & a_{22} & \cdots & a_{2m} \\ \vdots & \vdots & \ddots & \vdots \\ a_{m1} & a_{m2} & \cdots & a_{mm} \end{bmatrix} \tag{10}$$

Katz and Plotkin [2] introduced, what he called, the right hand side (RHS) of the equations, which are related to the components of the velocities due to the wing movement along the collocation points ($[U(t), V(t), W(t)]_k$), and to the components of the wake induced velocities ($(u_W, v_W, w_W)_k$) on that same point. The right hand side (RHS) of the equation for a collocation point k is given by

$$RHS_k = -\left[U(t) + u_W, V(t) + v_W, W(t) + w_W\right]_k \cdot \mathbf{n}_k = 0 \tag{11}$$

Once the influence coefficients and the righ hand side vectors (**RHS**) are computed, the follow system of algebric equations arises:

$$\begin{bmatrix} a_{11} & a_{12} & \cdots & a_{1m} \\ a_{21} & a_{22} & \cdots & a_{2m} \\ a_{31} & a_{32} & \cdots & a_{3m} \\ \vdots & \vdots & \ddots & \vdots \\ a_{m1} & a_{m2} & \cdots & a_{mm} \end{bmatrix} \begin{pmatrix} \Gamma_1 \\ \Gamma_2 \\ \Gamma_3 \\ \vdots \\ \Gamma_m \end{pmatrix} = \begin{pmatrix} RHS_1 \\ RHS_2 \\ RHS_3 \\ \vdots \\ RHS_m \end{pmatrix} \tag{12}$$

Reordering eq. (12), the problem that have to be solved is found:

$$\mathbf{\Gamma} = \mathbf{AIC}^{-1}\mathbf{RHS} \tag{13}$$

The circulation of each panel is found for each time step solving equation eq. (13), and the wing panels pressure distribution is determined. The methodology introduced here is described by Katz and Plotkin [2], and is based on the non-stationary Bernoulli equation. The pressure distribution of the panel ij is equal to:

$$\begin{aligned} \Delta p_{ij} = \rho \Bigg\{ & \left[U(t) + u_W, V(t) + v_W, W(t) + w_W\right]_{ij} \cdot \boldsymbol{\tau_i} \frac{\Gamma_{i,j} - \Gamma_{i-1,j}}{\Delta c_{i,j}} \\ & + \left[U(t) + u_W, V(t) + v_W, W(t) + w_W\right]_{ij} \cdot \boldsymbol{\tau_j} \frac{\Gamma_{i,j} - \Gamma_{i,j-1}}{\Delta b_{i,j}} + \frac{\partial}{\partial t}\Gamma_{ij} \Bigg\} \end{aligned} \tag{14}$$

where Δc_{ij} and Δb_{ij} are, respectively, the chordwise and spanwise panel length, $\boldsymbol{\tau_i}$ and $\boldsymbol{\tau_j}$ are the chordwise and spanwise tangent vectors and Δp_{ij} is the pressure distribution for each wing panel. Therefore, It's possible to determine the lift that each wing panel generate [2].

$$\Delta L_{ij} = \Delta p_{ij} S_{ij} \cos \alpha_{ij} \tag{15}$$

where S_{ij} is the panel area and α_{ij} the angle of attack.

Once the structural-dynamic and the aerodynamic models are defined, It's necessary to couple them to obtain the aeroelastic response of the wing. The methodology applied for the coupling of those two models is described with details on Benini [9] works. Next topic discuss briefly the coupling mechanism.

4 Coupling Between Aerodynamic and Structural Models

The mode shapes and the aerodynamic forces are defined using different meshes, so it is necessary to convert the aerodynamic forces to the structural points and to supply the structural displacements to the aerodynamic points. The aerodynamic and structural points are related through a coordinate transformation matrix ($\boldsymbol{G}$), and this matrix can be applied to write the mode shapes in terms of the aerodynamic points, according to eq. (16), where the subscript a is related to the aerodynamic points and s to the structural points [9].

$$\boldsymbol{\Phi}_a = \boldsymbol{G}\boldsymbol{\Phi}_s \tag{16}$$

Also it is possible to write the aerodynamic forces in terms of the structural points using the same coordinate transformation matrix.

$$\boldsymbol{L}_s = \boldsymbol{G}^T \boldsymbol{L}_a \tag{17}$$

Substituting eq. (17) into eq. (7) and making use of eq. (16) yields eq. (18), which represents the conversion of forces between the two meshes.

$$\ddot{\boldsymbol{\eta}}_s(t) + \omega^2 \boldsymbol{\eta}_s(t) = \boldsymbol{\Phi}_a^T \boldsymbol{L}_a \tag{18}$$

This equation is solved iteratively applying a predictor-corrector method, which is described by Benini [9], and the modal displacements ($\boldsymbol{\eta}$), that represents the wing response, are found.

As the UVLM provides the results in a time domain basis, to obtain the velocity-damping-frequency (V-g-f) plots it's necessary to apply a system identification method. This makes possible, starting from the frequency spectrum's of the time response, to obtain the damped natural frequencies and the respective damping ratios for each velocity. Analyzing the point where the damping ratio is null, it's possible to determine the flutter speed and frequency.

The modal parameter identification method applied in this work is the Least-Squares Complex Frequency (LSCF), described by Guillaume et al. [3]. This method is a implementation in the frequency domain of the well known Least-Squares Complex Exponential (LSCE). The main advantage of the LSCF over the LSCE, is the fact that it provides a fast stabilization, what makes it a efficient tool to find the modal parameters. All the theory involved and the numerical implementation procedure for the modal parameter identification method applied in this work are presented by Guillaume et al. [3].

5 Results and Discussion

On Modaress-Aval et al. [1] work, the aeroelastic analysis of cantilever rectangular plates with different aspect ratios (AR), that represents wings in a simplified way, was made. Both structural beam and plate models and Peters aerodynamic model were applied . The wings proposed are made of a homogeneous and isotropic material, and the AR varies from 6 to 16. For the thickness relation $L/h = 400$ was maintained, been L the semi-span and h the thickness. Table 1 shows the plate's properties.

The first step for the aeroelastic analysis, is to conduct the modal analysis. Here, a beam structural FEM model, developed by the authors, and the plate model developed by Gruppioni [8] were applied. The results obtained for the natural frequencies are compared to the ones obtained by Modaress-Aval et al. [1] using plate elements on the MSC Nastran, and are shown in Table 2 for three different aspect ratios: 8, 12, 16.

Analyzing Table 2, it's possible to observe that for the beam model, the differences on the natural frequencies for the three AR are similar and are between $5 - 7\%$, observing a higher difference for the torsion mode. It was expected lower differences for the plate model, but was observed that those differences are between 3% and 5%. Because of that a analysis was performed in ANSYS, considering

Table 1. Plate Properties and Aeroelastic Input Parameters

Plate Properties	
Semi-Span (m)	6, 8, 10, 12, 14, 16
Chord (m)	1
Thickeness (m)	0.015; 0.02; 0.025; 0.03; 0.035; 0.04
Material Density (kg/m^3)	2700
Modulus of Elasticity (GPa)	70
Poisson's Coefficient	0.3462
Air Density (kg/m^3)	1.225 (Sea Level)

Aeroelastic Input Parameters	
Chord (m)	1
Span (m)	6, 8, 12, 16
Velocity (m/s)	10 - 80
Angle of Attack (Degrees)	5
Air Density (kg/m^3)	1.225
Chordwise Panels	4
Spanwise Panels	13
Time Step (Seconds)	0.001
Total Iterations	10001
Total Time (Seconds)	10
Number of Modes	5

Table 2. Modal Analysis

		Modaress-Aval et al. (2020)	**Beam Model**		**Plate Model**	
	Mode	**MSC Nastran (Hz)**	**FEM (Hz)**	**Diff. (%)**	**FEM (Hz)**	**Diff (%)**
AR8	**1st Mode (Bending)**	0.2709	0.2570	-5.12%	0.2601	-3.97%
	2nd Mode (Bending)	1.6963	1.6108	-5.04%	1.6303	-3.89%
	3rd Mode (Torsion)	4.1285	3.8537	-6.66%	4.0101	-2.87%
	4th Mode (Bending)	4.7556	4.5104	-5.16%	4.5770	-3.76%
	5th Mode (Bending)	9.3432	8.8385	-5.40%	9.0112	-3.55%
AR12	**1st Mode (Bending)**	0.1810	0.1713	-5.37%	0.1729	-4.49%
	2nd Mode (Bending)	1.1341	1.0738	-5.32%	1.0837	-4.44%
	3rd Mode (Bending)	3.1776	3.0069	-5.37%	3.0387	-4.37%
	4th Mode (Torsion)	4.1070	3.8404	-6.49%	3.9664	-3.42%
	5th Mode (Bending)	6.2357	5.8923	-5.51%	5.9711	-4.24%
AR16	**1st Mode (Bending)**	0.1361	0.1285	-5.60%	0.1295	-4.87%
	2nd Mode (Bending)	0.8528	0.8054	-5.56%	0.8116	-4.83%
	3rd Mode (Bending)	2.3888	2.2551	-5.60%	2.2747	-4.78%
	4th Mode (Torsion)	4.1031	3.8268	-6.73%	3.9456	-3.84%
	5th Mode (Bending)	4.6852	4.4192	-5.68%	4.4657	-4.68%

the structure discretized in beam and plate elements, to ratify those results. The results are presented in Table 3.

Table 3. Modal Analysis - ANSYS

		Beam Model			**Plate Model**		
	Mode	**Ansys (Hz)**	**FEM Code (Hz)**	**Diff. (%)**	**Ansys (Hz)**	**FEM Code (Hz)**	**Diff. (%)**
AR8	**1st Mode (Bending)**	0.2570	0.2570	-0.02%	0.2600	0.2601	0.05%
	2nd Mode (Bending)	1.6108	1.6108	0.00%	1.6287	1.6303	0.10%
	3rd Mode (Torsion)	3.8757	3.8537	-0.57%	4.0023	4.0101	0.19%
	4th Mode (Bending)	4.5100	4.5104	0.01%	4.5699	4.5770	0.16%
	5th Mode (Bending)	8.8372	8.8385	0.01%	8.9891	9.0112	0.25%
AR12	**1st Mode (Bending)**	0.1714	0.1713	-0.04%	0.1727	0.1729	0.13%
	2nd Mode (Bending)	1.0738	1.0738	0.00%	1.0820	1.0837	0.16%
	3rd Mode (Bending)	3.0067	3.0069	0.01%	3.0327	3.0387	0.20%
	4th Mode (Torsion)	3.8717	3.8404	-0.81%	3.9498	3.9664	0.42%
	5th Mode (Bending)	5.8914	5.8923	0.02%	5.9541	5.9711	0.29%
AR16	**1st Mode (Bending)**	0.1285	0.1285	-0.02%	0.1293	0.1295	0.19%
	2nd Mode (Bending)	0.8054	0.8054	0.00%	0.8100	0.8116	0.20%
	3rd Mode (Bending)	2.2550	2.2551	0.00%	2.2693	2.2747	0.24%
	4th Mode (Torsion)	3.8661	3.8268	-1.02%	3.9182	3.9456	0.70%
	5th Mode (Bending)	4.4186	4.4192	0.01%	4.4518	4.4657	0.31%

From Table 3, it's possible to observe that the differences for both beam and plate finite element formulation are quite lower when comparing to the ones obtained with ANSYS, which validates the models applied here for the structural analysis. The differences between the plate results and the results obtained by Modaress-Aval et al. [1] are beeing investigated, but, as will be discussed further in this topic, it affected the aeroelastic analysis results. More tests have to be conducted to confirm the causes of those discrepancies.

Once the modal analysis was conduct, the natural frequencies and mode shapes serves as input for the aerodynamic and aeroelastic solvers. It's important to emphasize that the results obtained for the beam elements mode shapes were interpolated to represent the 3D vibration pattern of the wing according to the chosen aerodynamic mesh grid. Also, the structural and aerodynamic models ares coupled together according to the procedure described in section 4. The input parameters for the aeroelastic analysis are shown on Table 1. It's important to emphasize that in this work only the wings with AR 6, 8, 12 and 16 are beeing analyzed.

It's possible to observe on Table 1 that the mesh defined is 4×13, and the time step (Δt) is equal to 0.001 seconds. Also, only the first five vibration modes were used in the analysis. As the UVLM works in a time domain basis, the results obtained are the time histories of the wing displacements. For the wing with AR8, and considering the structural beam and plate models, the time responses and power spectrum densities (PSD) for the velocity equals to 40m/s and 60m/s are presented, respectively, on Fig. 2 and Fig. 3.

Figure 2. Time Response - AR8 - $V = 40m/s$

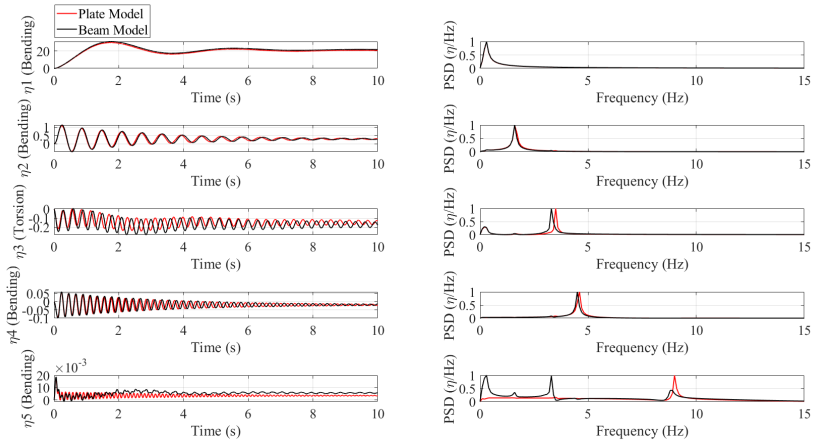

Figure 3. Time Response - AR8 - $V = 60m/s$

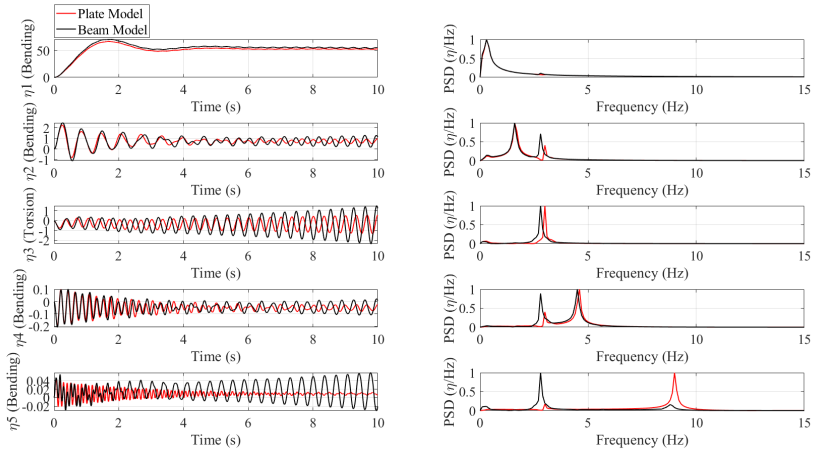

From Fig. 2 and Fig. 3, it's possible to visualize graphically that the flutter speed is between 40 and 60 m/s for the wing with AR 8 considering the beam and the plate model. Also, differences between

those two structural models on the aeroelastic analysis are noted. For the beam model, the flutter occurs in a lower speed when comparing to the plate model. Despite that, the flutter frequencies are quite close.

To assess the flutter speeds and frequencies with precision, the Least-Squares Complex Frequency [3], a modal parameter identification method, was applied. It provides, from the Power Spectrum Densities as inputs, the damped natural frequencies and damping ratios for each velocity. From those informations, the velocity-damping-frequency (V-g-f) charts are obtained. From them, it's possible to determine the null damping ratio point, which indicates where the flutter occurs. Fig. 4 shows the V-g-f's for the wing with aspect ratio 8 considering both plate and beam structural models.

Figure 4. V-g-f - AR8

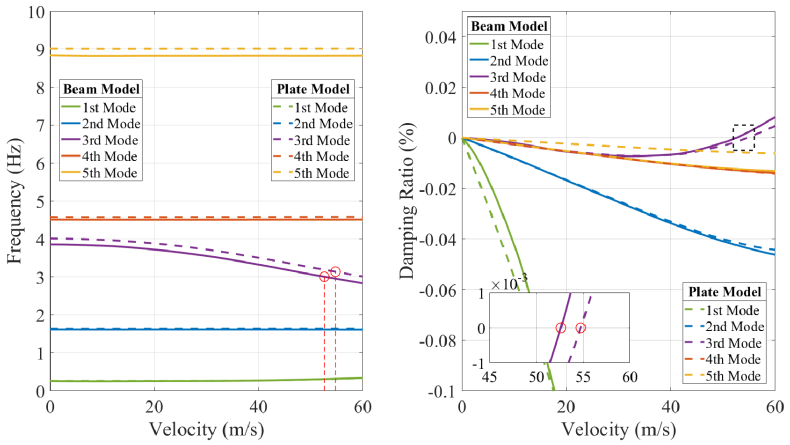

From the V-g-f, it's possible to identify that the flutter speed and frequency for the beam structural discretization of the AR 8 wing are, respectively, $52.61 m/s$ and $3.003 Hz$. For the plate discretization, the flutter speed and frequency are $54.73 m/s$ and $3.1359 Hz$. It was possible to confirm what was observed on the time responses and frequency spectrums illustrated at Fig. 2 and Fig. 3, i.e., the flutter speed is higher considering the plate model on the aeroelastic analysis, and the flutter frequencies are quite close.

This procedure was repeated for the wings with aspect ratios equals to 6, 12 and 16. The results for the flutter speed are presented on Table 4.

Table 4. Flutter Speed (m/s)

Aspect Ratio	Beam Model			Plate Model		
	Modaress-Aval et. al (2020)	Present Work	Diff (%)	Modaress-Aval et. al (2020)	Present Work	Diff. (%)
6	44.64	45.64	2,24%	50.36	47.58	-5.52%
8	51.41	52.61	2,33%	56.99	54.73	-3.96%
12	62.32	61.24	-1.72%	68.82	62.81	-8.73%
16	71.24	68.01	-4.53%	76.94	71.40	-7.20%

From Table 4, it's possible to observe an increase on the flutter speed value with the increase of the aspect ratio, what is illustrated on Fig. 5. Comparing the results obtained in the present work, with the ones obtained by Modaress-Aval et al. [1], it's observed that, despite the differences, a good agreement have been achieved. For the plate model, those differences were higher than the ones found for the beam model. The modal analysis conducted by Modaress-Aval et al. [1] on the MSC Nastran maybe influenced the aeroelastic results, given the discrepancies between this analysis and the one conduct on ANSYS. Also, the different aerodynamic models used, UVLM in the present work and Peters model in Modaress-Aval et al. [1], may incur in differences.

6 Conclusion

Despite the points highlighted here, the results obtained analyzing the case study proposed by Modaress-Aval et al. [1], mainly considering the structural beam model, which is the main focus of this work, were quite promising. It's possible to say that the models applied here, both structural, aeroelastic

Figure 5. Flutter Speed X Aspect Ratio

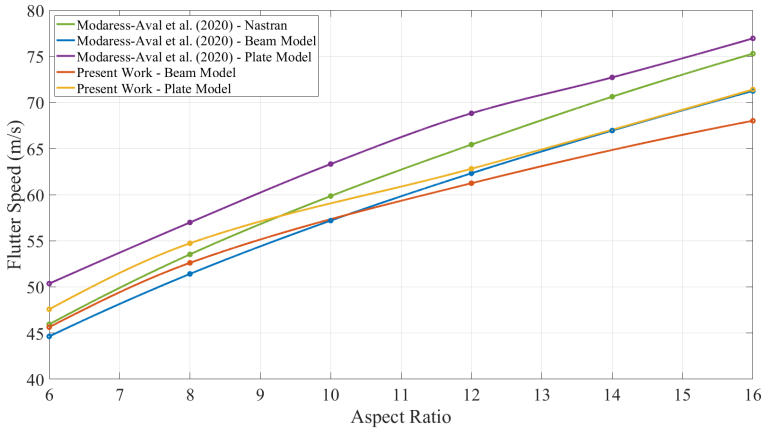

and system identification, have a good accuracy for the determination of natural frequencies and mode shapes, and for the flutter prediction.

The discrepancies are being investigated and further analysis will be conducted. One of the main hypothesis for that differences is that the aerodynamic mesh was kept constant for all aspect ratios, therefore, higher the AR, higher the plate spanwise length, what can decrease the efficiency of the aeroelastic solver.

Acknowledgements. This study was carried out with the financial support of the Conselho Nacional de Desenvolvimento Científico e Tecnológico (National Council for Scientific and Technological Development) - CNPQ (130984/2021-3).

Authorship statement. The authors hereby confirm that they are the sole liable persons responsible for the authorship of this work, and that all material that has been herein included as part of the present paper is either the property (and authorship) of the authors, or has the permission of the owners to be included here.

References

[1] A. H. Modaress-Aval, F. Bakhtiari-Nejad, E. H. Dowell, H. Shahverdi, H. Rostami, and D. Peters. Aeroelastic analysis of cantilever plates using peters' aerodynamic model, and the influence of choosing beam or plate theories as the structural model. *Journal of Fluids and Structures*, vol. 96, pp. 103010, 2020.

[2] J. Katz and A. Plotkin. *Low-speed Aerodynamics: From Wing Theory to Panel Methods*. McGraw-Hill Series in Population Biology. McGraw-Hill, 1991.

[3] P. Guillaume, P. Verboven, S. Vanlanduit, Van der H. Auweraer, and B. Peeters. A poly-reference implementation of the least-squares complex frequency-domain estimator. *Proceedings of IMAC*, vol. 21, 2003.

[4] R. Cook and H. Saunders. Concepts and applications of finite element analysis, 1984.

[5] R. Craig and A. Kurdila. *Fundamentals of Structural Dynamics*. Wiley, 2006.

[6] J. N. Reddy. *Introduction to the finite element method*. McGraw-Hill Education, 2019.

[7] J. Katsikadelis. *Dynamic Analysis of Structures*. Elsevier Science, 2020.

[8] E. M. Gruppioni. *Controle aeroelástico por lógica difusa de uma asa flexível não-linear com atuadores piezelétricos incorporados*. (tese de doutorado), Universidade de São Paulo (USP). Escola de Engenharia de São Carlos (EESC), São Carlos, 2008.

[9] G. R. Benini. Modelo numérico para simulação da resposta aeroelástica de asas fixas, 2002.